

# Low Latency Privacy Preserving Inference

Alon Brutzkus

Microsoft Research and Tel Aviv University  
alonbrutzkus@mail.tau.ac.il

Oren Elisha  
Microsoft

orelisha@microsoft.com

Ran Gilad-Bachrach  
Microsoft Research

rang@microsoft.com

November 14, 2021

## Abstract

When applying machine learning to sensitive data, one has to balance between accuracy, information leakage, and computational-complexity. Recent studies have shown that Homomorphic Encryption (HE) can be used for protecting against information leakage while applying neural networks. However, this comes with the cost of limiting the width and depth of neural networks that can be used (and hence the accuracy) and with latency of the order of several minutes even for relatively simple networks. In this study we provide two solutions that address these limitations. In the first solution, we present more than  $10\times$  improvement in latency and enable inference on wider networks compared to prior attempts with the same level of security. The improved performance is achieved via a collection of methods to better represent the data during the computation. In the second solution, we apply the method of transfer learning to provide private inference services using deep networks with latency less than 0.2 seconds. We demonstrate the efficacy of our methods on several computer vision tasks.

## 1 Introduction

Machine learning is used in domains such as education, health, and finance in which data may be private or confidential. Therefore, machine learning algorithms should preserve privacy while making accurate predictions. The privacy requirement pertains to all sub-tasks of the learning process, such as training and inference. In this work, we focus on private neural-networks inference. In this problem, popularized by the work on CryptoNets (Dowlin et al., 2016), the goal is to build an inference service that can make predictions on private data. To achieve this goal, the data is encrypted before it is sent to the prediction service which should be capable of operating on the encrypted data without having access to the raw content. To allow that, several cryptology technologies have been proposed, including Secure Multi-Party Computation (MPC) (Yao, 1982; Goldreich et al., 1987), hardware enclaves, such as Intel’s Software Guard Extensions (SGX) (McKeen et al., 2013), Homomorphic Encryption (Gentry, 2009), and combinations of these techniques.

The different approaches present different trade-offs in terms of computation, accuracy, and security. HE presents the most stringent security model. The security assumption relies on the hardness of solving a mathematical problem for which there are no known efficient algorithms, even in the presence of quantum computers (Gentry, 2009; Albrecht et al., 2018). Other techniques, such

as MPC and SGX make additional assumptions and therefore provide a weaker sense of protection to the data (Yao, 1982; McKeen et al., 2013; Chen et al., 2018; Koruyeh et al., 2018).

While HE provides the highest level of security it is also limited in the kind of operations it allows and the complexity of these operations (see Section 1.1). CryptoNets (Dowlin et al., 2016) was the first demonstration that it may be feasible to use HE to build privacy preserving Encrypted Prediction as a Service (EPaaS) solutions (Sanyal et al., 2018). CryptoNets are capable of making predictions with accuracy of 99% on the MNIST task (LeCun et al., 2010) such that each prediction takes 250 seconds to complete. CryptoNets are also capable of packing 4096 prediction requests and operate on all of them in parallel which allows throughput of  $\sim 59000$  predictions per hour.

CryptoNets have several limitations that we address in this work, the first of them is latency. CryptoNets provide high throughput by operating on 4096 instances in parallel, however, all these instances have to come from a single source and use the same secret key. Therefore, this capability may be of little use in practice. Thus, we trade the high throughput in favor of low latency and show that the same neural network that was used by CryptoNets can be evaluated in as little as 2.2 seconds. We show that a part of this gain is an “engineering gain” which is a result of using a more recent implementation of HE. However, this “engineering gain” accounts for only  $10\times$  speedup. Most of the speedup comes from a new way to represent data when applying neural-networks using HE which we call LoLa. In a nut-shell, CryptoNets represent each node in the neural network as a separate message for encryption, while LoLa encrypts entire layers which results in a  $11.2\times$  speedup on top of the “engineering gain”. Together, these improvements results in a  $114\times$  improvement in latency while maintaining the same level of security and accuracy.<sup>1</sup>

LoLa provides another significant benefit over CryptoNets. Since CryptoNets encode every node in the network as a separate message, they create a memory bottleneck when applied to networks with many nodes. We demonstrate that in an experiment conducted on the CIFAR-10 dataset for which the CryptoNets approach fails to execute since it requires 100’s of Gigabytes of RAM. However, the low-latency approach, LoLa, which encodes layers instead of nodes, can make predictions in 12 minutes using only few Gigabytes of RAM.

The experiment on CIFAR demonstrates that the LoLa approach can handle larger networks than CryptoNets. However, there is still a big penalty for the size of the network: predictions on MNIST are achieved in 2.2 seconds, and this latency jumps to 12 minutes for the slightly more complex task in the CIFAR-10 dataset. Therefore, it is reasonable to ask whether any of these approaches can scale to handle tasks such as analyzing large and complex images. To that extent, we propose another solution which represents the input to the network using semantically meaningful features instead of pixels. These semantically meaningful features are extracted using the convolution layers of standard networks such as AlexNet (Krizhevsky et al., 2012). We consider these networks as “standard libraries” for machine learning tasks. Using such features allows reducing the size of the message to be sent and the complexity of the network that is needed for classification. Indeed, we use this approach to demonstrate private predictions in 0.18 seconds on the CalTech-101 dataset with class balanced accuracy of 75.7%.

## 1.1 Homomorphic Encryption

In this work we use Homomorphic Encryptions (HE) to provide privacy (we refer the reader to Dowlin et al. (2017) for a more comprehensive introduction). HEs are encryptions that allow operating on data while it is encrypted without requiring access to the secret key (Gentry, 2009). The data used for encryption is assumed to be elements in a ring  $\mathcal{R}$ . On top of the encryption function  $\mathbb{E}$

---

<sup>1</sup>The HE scheme used by CryptoNets was found to have some weaknesses that the HE scheme that we use does not suffer from.

and the decryption function  $\mathbb{D}$ , the HE scheme provides two additional operators  $\oplus$  and  $\otimes$  such that for any  $x_1, x_2 \in \mathcal{R}$

$$\begin{aligned}\mathbb{D}(\mathbb{E}(x_1) \oplus \mathbb{E}(x_2)) &= x_1 + x_2 \text{ and} \\ \mathbb{D}(\mathbb{E}(x_1) \otimes \mathbb{E}(x_2)) &= x_1 \times x_2\end{aligned}$$

where  $+$  and  $\times$  are the standard addition and multiplication operations on the ring  $\mathcal{R}$ . Therefore, the  $\oplus$  and  $\otimes$  operators allow computing addition and multiplication operators on the data in its encrypted form and thus computing any polynomial function.

Since Gentry’s seminal paper, in which he introduced the first HE scheme (Gentry, 2009), additional schemes have been proposed. In this work we use the Brakerski/Fan-Vercauteren scheme (BFV) (Fan & Vercauteren, 2012; Brakerski & Vaikuntanathan, 2014) as it is implemented in the SEAL library version 2.3.1.<sup>2</sup> In this scheme, the ring on which the Homomorphic Encryption operates is  $\mathcal{R} = \frac{\mathbb{Z}_p[x]}{x^n+1}$  where  $\mathbb{Z}_p = \frac{\mathbb{Z}}{p\mathbb{Z}}$ . If the parameters  $p$  and  $n$  are chosen such that there is an order  $2n$  root of unity in  $\mathbb{Z}_p$ , then every element in  $\mathcal{R}$  can be viewed as a vector of dimension  $n$  of elements in  $\mathbb{Z}_p$  where addition and multiplication operate component-wise (Brakerski et al., 2014). In this view, the BFV scheme allows a another operation on the encrypted data: rotation. The ideal rotation operation of size  $k$  sends the value in the  $i$ ’th coordinate of a vector to the  $((i+k) \bmod n)$  coordinate. The BFV scheme allows a slight modified version of the ideal rotation (see Appendix A) but for the sake of our discussion this detail is insignificant.

## 1.2 Related Work

The task of private predictions gained significant attention in recent years. Dowlin et al. (2016) presented CryptoNets which demonstrated the feasibility of private neural networks predictions using HE. CryptoNets are capable of making predictions with high throughput but are limited in both the depth of the network they can support and the latency per prediction. Bourse et al. (2017) used a different HE scheme that allows fast bootstrapping which results in only linear penalty for additional layers in the network. However, it is slower per operation and therefore, the results they presented on the MNIST data-set use small models with significantly lower accuracy (see Table 1). Recently, Boemer et al. (2018) proposed an HE based extension to the Intel nGraph compiler. They use the same techniques as Cryptonets (Dowlin et al., 2016) and use the HEAAN encryption scheme (Cheon et al., 2017). Their solution is slower than ours in terms of latency (see Table 1). Sanyal et al. (2018) argued that many of these methods leak information about the structure of the neural-network that the service provider uses through the parameters of the encryption. They presented a method that leaks less information about the neural-network but their solution is orders of magnitude slower. Nevertheless, their solution has the nice benefit that it allows the service provider to change the network without requiring changes in the client side.

Other researchers proposed using different encryption schemes. For example, the Chameleon system (Riazi et al., 2018) uses MPC to demonstrate private predictions on MNIST and Juvekar et al. (2018) use a hybrid MPC-HE approach for the same task. Hardware based solutions were also proposed, for example, Tramer & Boneh (2018). Some of these approaches provide faster predictions which are, in some cases, more accurate, however, this comes with the cost of a using a lower level of security.

<sup>2</sup>The SEAL library can be found at <http://sealcrypto.org/>. We use parameters that guarantee 128 bits of security according to the proposed standard for Homomorphic Encryptions (Albrecht et al., 2018).

## 2 Data Representation

Feed-forward neural networks are functions that can be computed by an alternating sequence of linear transformations and non-linear transformations. Linear transformations include dense, convolution layers and average pooling layers. Non-linear transformations include activation functions and max pooling layers. In most cases, we can consider this sequence to be alternating between linear transformations and non-linear ones since consecutive linear transformations can be combined into a single linear transformation and sequences of non-linear transformations can be merged as well.

For most of this work, we restrict the non-linear transformations to the square activation function. This follows CryptoNets (Dowlin et al., 2016) that showed that high accuracy can be achieved even with this restriction. We demonstrate this again on the CIFAR data-set in Section 4. Recall that HE supports point-wise multiplication of vectors and therefore it is straight-forward to implement the square activation function.

The main linear transformations we consider are dot-products and matrix-vector multiplications. Given two vectors, we can implement a dot product between two vectors whose size is a power of 2 by first applying point-wise multiplication between the two vectors and then a series of  $\log n$  rotations of size 1, 2, 4,  $\dots$ ,  $n/2$  and addition between each rotation. The result of such a dot product operation is a vector that holds the results of the dot-product in all its coordinates.<sup>3</sup>

The dot-product operation can induce a change in representations. For example, given a weights matrix and an input vector represented as a single message, we can multiply the matrix by the vector using  $r$  dot-product operations where  $r$  is the number of rows in the matrix. The result of this operation is a vector of length  $r$  that is spread across  $r$  messages. Therefore, the result has a different representation than the representation of the input vector. Different representations can induce different computational costs and therefore choosing the right representations throughout the computation is important for computational efficiency. It is possible to change representations but this requires additional computational steps. Instead, we propose using various representations in the network inference. We start our discussion by presenting different possible vector representations.

### 2.1 Vector representations

Recall that a message in HE can be thought of as a vector of length  $n$  of elements in  $\mathbb{Z}_p$ . For the sake of brevity, we assume that the dimension of the vector  $\mathbf{v}$  to be encoded is of length  $k$  such that  $k \leq n$ , for otherwise multiple messages can be combined. For any vector  $\mathbf{u}$  we denote by  $u_i$  its  $i^{\text{th}}$  coordinate.

**2.1.1 Dense representation:** A vector  $\mathbf{v}$  is represented as a single message  $\mathbf{m}$  by setting  $v_i \mapsto m_i$ .

**2.1.2 Sparse representation:** A vector  $\mathbf{v}$  of length  $k$  is represented in  $k$  messages  $\mathbf{m}^1, \dots, \mathbf{m}^k$  such that  $\mathbf{m}^i$  is a vector in which every coordinate is set to  $v_i$ .<sup>4</sup>

<sup>3</sup>For example, consider calculating the dot product of 4-dimensional vectors  $(v_1, \dots, v_4)$  and  $(w_1, \dots, w_4)$ . Point-wise multiplication, rotation of size 1 and summation results in the vector  $(v_1w_1 + v_4w_4, v_2w_2 + v_1w_1, v_3w_3 + v_2w_2, v_4w_4 + v_3w_3)$ . Another rotation of size 2 and summation results in the 4 dimensional vector which contains the dot-product of the vectors in all coordinates.

<sup>4</sup>Recall that the encrypted messages are in the ring  $R = \frac{\mathbb{Z}_p[x]}{x^n+1}$  which, by the choice of parameters, is homomorphic to  $(\mathbb{Z}_p)^n$ . When a vector has the same value  $v_i$  in all its coordinates, then its polynomial representation in  $\frac{\mathbb{Z}_p[x]}{x^n+1}$  is the constant polynomial  $v_i$ .

**2.1.3 Stacked representation:** For a short (low dimension) vector  $\mathbf{v}$ , the stacked representation holds several copies of the vector  $\mathbf{v}$  in a single message  $\mathbf{m}$ . Typically this will be done by finding  $d = \lceil \log(k) \rceil$ , the smallest  $d$  such that the dimension of  $\mathbf{v}$  is at most  $2^d$  and setting  $m_i, m_{i+2^d}, m_{i+2 \cdot 2^d}, \dots = v_i$ .

**2.1.4 Interleaved representation:** The interleaved representation uses a permutation  $\sigma$  of  $[1, \dots, n]$  to set  $m_{\sigma(i)} = v_i$ . The dense representation can be viewed as a special case of the interleaved representation where  $\sigma$  is the identity permutation.

**2.1.5 Convolution representation:** This is a special representation that makes convolution operations efficient. A convolution, when flattened to a single dimension, can be viewed as a restricted linear operation where there is a weight vector  $\mathbf{w}$  of length  $r$  (the window size) and a set of permutations  $\sigma_i$  such that the  $i$ 'th output of the linear transformation is  $\sum_j w_j v_{\sigma_i(j)}$ . The convolution representation takes a vector  $v$  and represents it as  $r$  messages  $\mathbf{m}^1, \dots, \mathbf{m}^r$  such that  $m_i^j = v_{\sigma_i(j)}$ .<sup>5</sup>

**2.1.6 SIMD representation:** CryptoNets (Dowlin et al., 2016) represent each data element as a separate message but maps multiple data vectors into the same set of messages. More details about this representation are in Appendix B.

## 2.2 Matrix-vector multiplications

Matrix-vector multiplication is a core operation in neural networks. The matrix may contain the learned weights of the network and the vector represents the values of the nodes at a certain layer. Here we present different ways to implement such matrix-vector operations. Each method operates on vectors in different representations and produces output in yet another representation. Furthermore, the weight matrix has to be represented appropriately as a set of vectors, either column-major or row-major to allow the operation. We assume that the matrix  $W$  has  $k$  columns  $\mathbf{c}^1, \dots, \mathbf{c}^k$  and  $r$  rows  $\mathbf{r}^1, \dots, \mathbf{r}^r$ .

**2.2.1 Dense Vector – Row Major:** If the vector is given as a dense vector and each row  $\mathbf{r}^j$  of the weight matrix is encoded as a dense vector then the matrix-vector multiplication can be applied using  $r$  dot-product operations. As already described above, a dot-product requires a single multiplication and  $\log(n)$  additions and rotations. The result is a sparse vector of length  $r$ .

**2.2.2 Sparse Vector – Column Major:** Recall that  $W\mathbf{v} = \sum v_i \mathbf{c}^i$ . Therefore, when  $\mathbf{v}$  is encoded in a sparse format, the message  $\mathbf{m}^i$  has all its coordinate set to  $v_i$  and  $v_i \mathbf{c}^i$  can be computed using a single point-wise multiplication. Therefore,  $W\mathbf{v}$  can be computed using  $k$  multiplications and additions and the result is a dense vector.

<sup>5</sup>For example, consider a matrix  $A \in \mathbb{R}^{4 \times 4}$  which corresponds to an input image and a  $2 \times 2$  convolution filter that slides across the image with stride 2 in each direction. Let  $a_{i,j}$  be the entry at row  $i$  and column  $j$  of the matrix  $A$ . Then, in this case  $r = 4$  and the following messages are formed  $M^1 = (a_{1,1}, a_{1,3}, a_{3,1}, a_{3,3})$ ,  $M^2 = (a_{1,2}, a_{1,4}, a_{3,2}, a_{3,4})$ ,  $M^3 = (a_{2,1}, a_{2,3}, a_{4,1}, a_{4,3})$  and  $M^4 = (a_{2,2}, a_{2,4}, a_{4,2}, a_{4,4})$ . In some cases it will be more convenient to combine the interleaved representation with the convolution representation by a permutation  $\tau$  such that  $m_{\tau(i)}^j = v_{\sigma_i(j)}$ .

**2.2.3 Stacked Vector – Row Major:** For the sake of clarity, assume that  $k = 2^d$  for some  $d$ . In this case  $n/k$  copies of  $\mathbf{v}$  can be stacked in a single message  $\mathbf{m}$  (this operation requires  $\log(n/k) - 1$  rotations and additions). By concatenating  $n/k$  rows of  $W$  into a single message a special version of the dot-product operation can be used to compute  $n/k$  elements of  $W\mathbf{v}$  at once. First, a point-wise multiplication of the stacked vector and the concatenated rows is applied followed by  $d - 1$  rotations and additions where the rotations are of size  $1, 2, \dots, 2^{d-1}$ . The result is in the interleaved representation.<sup>6</sup>

The Stacked Vector - Row Major gets its efficiency from two places. First, the number of modified dot product operations is  $n/k$  and each dot product operation requires a single multiplication and second, only  $d$  rotations and additions (compared to  $\log n$  rotations and additions in the standard dot-product procedure).

**2.2.4 Interleaved Vector – Row Major:** This setting is very similar to the dense vector – row major matrix multiplication procedure with the only difference being that the columns of the matrix have to be shuffled to match the permutation of the interleaved representation of the vector. The result is in sparse format.

**2.2.5 Convolution vector – Row Major:** A convolution layer applies the same linear transformation to different locations on the data vector  $\mathbf{v}$ . For the sake of brevity, assume the transformation is one-dimensional. In neural network language that would mean that the kernel has a single map. Obviously, if more maps exist, then the process described here can be repeated multiple times.

Recall that a convolution, when flattened to a single dimension, is a restricted linear operation where the weight vector  $\mathbf{w}$  is of length  $r$ , and there exists a set of permutations  $\sigma_i$  such that the  $i$ 'th output of the linear transformation is  $\sum w_j v_{\sigma_i(j)}$ . In this case, the convolution representation is made of  $r$  messages such that the  $i$ 'th element in the message  $\mathbf{m}^j$  is  $v_{\sigma_i(j)}$ . By using a sparse representation of the vector  $\mathbf{w}$ , we get that  $\sum w_j \mathbf{m}^j$  computes the set of required outputs using  $r$  multiplications and additions. When the weights are not encrypted, the multiplications used here are relatively cheap since the weights are scalar and BFV supports fast implementation of multiplying a message by a scalar. The result of this operation is in a dense format.

### 3 Secure Networks for MNIST

The neural network used for the MNIST data-set (LeCun et al., 2010) is the same network used by CryptoNets (Dowlin et al., 2016). After suppressing adjacent linear layers it can be presented as a  $5 \times 5$  convolution layer with a stride of  $(2, 2)$  and 5 output maps, which is followed by a square activation function that feeds a fully connected layer with 100 output maps, another square activation and another fully connected layer with 10 outputs (see Figure 2 in the appendix).

The baseline implementation uses the techniques presented in CryptoNets in Table 1. Recall that CryptoNets use the SIMD representation (Section 2.1.6) in which each pixel requires its own message. Therefore, since each image in the MNIST data-set is made of an array of  $28 \times 28$  pixels, the input to the CryptoNets network is made of 784 messages. On the reference machine used for this work (Azure standard B8ms virtual machine with 8 vCPUs and 32GB of ram) the original CryptoNets implementation runs in 205 seconds. Re-implementing it to use better memory management

<sup>6</sup>For example, consider a  $2 \times 2$  matrix  $W$  flattened to a vector  $\mathbf{w} = (w_{1,1}, w_{1,2}, w_{2,1}, w_{2,2})$  and a two-dimensional vector  $\mathbf{v} = (v_1, v_2)$ . Then, after stacking the vectors, point-wise multiplication, rotation of size 1 and summation, the second entry of the result contains  $w_{1,1}v_1 + w_{1,2}v_2$  and the fourth entry contains  $w_{2,1}v_1 + w_{2,2}v_2$ . Hence, the result is in an interleaved representation.

and multi-threading in SEAL 2.3 reduces the running time to 24.8 seconds. Since this implementation allows batching of 8192 images to be processed simultaneously, it has a potential throughput of 1189161 predictions per hour which is, as far as we know, the highest throughput reported on this task by a large margin.

While CryptoNets provide high throughput, in many cases, it is hard to utilize this high throughput which requires batching together 8192 requests from sources that share the same secret key. If each user has only a single record to be predicted on, the throughput is governed by the latency and therefore, we move towards reducing latency. We do that by replacing the SIMD representation with other representations. As a result, throughput is sacrificed in favor of latency.

The Low-Latency CryptoNets (LoLa) uses the same network layout and has accuracy of 98.95% (see Table 2 for a summary of the data representations used by LoLa). However, it is implemented differently: the input to the network is a single dense message where the pixel values are mapped to coordinates in the encoded vector line after line. The first step in processing this message is breaking it into 25 messages corresponding to the 25 pixels in the convolution map to generate a convolution representation. Creating each message requires a single vector multiplication. This is performed by creating 25 masks. The first mask is a vector of zeros and ones that corresponds to a matrix of size  $28 \times 28$  such that a one is in the  $(i, j)$  coordinate if the  $i, j$  pixel in the image appears as the upper left corner of the  $5 \times 5$  window of the convolution layer. Multiplying point-wise the input vector by the mask creates the first message in the convolution representation as described in Section 2.1.5 hybridized with the interleaved representation as described in footnote 5. Similarly the other messages in the convolution representation are created. Note that all masks are shifts of each other which allows using the convolution representation-row major multiplication to implement the convolution layer (see Section 2.2.5). To do that, think of the 25 messages as a matrix and the weights of a map of the convolution layer as a sparse vector. Therefore, the outputs of the entire map can be computed using 25 multiplications (of each weight by the corresponding vector) and 24 additions. Note that there are 169 windows and all of them are computed simultaneously. However, the process repeats 5 times for the 5 maps of the convolution layer.

The result of the convolution layer are 5 messages, each one of them contains 169 results. They are united into a single vector by rotating the messages such that they will not have active values in the same locations and summing the results. At this point, a single message holds all the 845 values (169 windows  $\times$  5 maps). This vector is squared, using a single multiplication operation, to implement the activation function that follows the convolution layer. This demonstrates one of the main differences between CryptoNets and LoLa; In CryptoNets, the activation layer requires 845 multiplication operations, whereas in LoLa it is a single multiplication. Even if we add the manipulation of the vector to place all values in a single message, as described above, we add only 4 rotations and 4 additions which are still much fewer operations than in CryptoNets.

Next, we apply a dense layer with 100 maps. LoLa uses messages of size  $n = 16384$  where the 845 results of the previous layer, even though they are in interleaving representation, take fewer than 1024 dimensions. Therefore, 16 copies are stacked together which allows the use of the Stacked vector – Row Major multiplication method. This allows computing 16 out of the 100 maps in each operation and therefore, the entire dense layer is computed in 7 iterations resulting in 7 interleaved messages. By shifting the  $i^{\text{th}}$  message by  $i - 1$  positions, the active outputs in each of the messages are no longer in the same position and they are added together to form a single interleaved message that contains the 100 outputs. The following square activation requires a single point-wise-multiplication of this message. The final dense layer is applied using the Interleaved vector – Row Major method to generate 10 messages, each of which contains one of the 10 outputs.<sup>7</sup>

<sup>7</sup> It is possible, if required, to combine them into a single message in order to save communication.

Method	Accuracy	Latency	Throughput	
FHE-DiNN100	96.35%	1.65	2182	(Bourse et al., 2017)
LoLa-Small	96.92%	<b>0.29</b>	12500	
CryptoNets	98.95%	250	58982	(Dowlin et al., 2016)
nGraph-HE	Unknown <sup>8</sup>	135	105883	(Boemer et al., 2018)
CryptoNets 2.3	98.95%	24.8	<b>1189160</b>	
LoLa	98.95%	7.2	500	
LoLa-Conv	98.95%	<b>2.2</b>	1636	

Table 1: MNIST performance comparison. Solutions are grouped by accuracy levels.

Overall, applying the entire network takes only 7.2 seconds on the same reference hardware which is  $34.7\times$  faster than CryptoNets and  $3.4\times$  faster than CryptoNets 2.3. This result can be further improved by changing the input to the network; Instead of taking as an input a dense representation of the image, the LoLa-Conv network takes as its input 25 messages which are the convolution representation of the image. This removes a processing step which saves time but also reduces the amount of noise accumulated during the computation and allows working with messages of size  $n = 8192$ , which further reduces the computation time. The LoLa-Conv starts with a convolution vector – row major multiplication for each of the 5 maps of the convolution layer. The 5 dense output messages are joined together with a rotation and addition to form a single dense vector of 845 elements. This vector is squared using a single multiplication and 8 copies of the results are stacked before applying the dense layer as 13 rounds of Stacked vector – Row Major multiplication. The 13 vectors of interleaved results are rotated and added to form a single interleaved vector of results which is squared using a single multiplication. Finally, Interleaved vector – Row Major multiplication is used to obtain the final result. This version computes the entire network in only 2.2 seconds which is  $3.3\times$  faster than LoLa,  $11\times$  faster than CryptoNets 2.3 and  $114\times$  faster than CryptoNets. See Table 3 for a summary of the data representations used by LoLa-Conv.

Table 1 shows a summary of the performance of different methods and more details can be found in Appendix C. Bourse et al. (2017) showed faster results with similar security level, albeit with lower accuracy. To compare with that, LoLa-Small is similar to Lola-Conv but has only a convolution layer, square activation and a dense layer. This solution is more accurate than the networks used by Bourse et al. (2017) and at the same time it is  $5.5\times$  faster.

## 4 Secure Networks for CIFAR

The Cifar-10 data-set (Krizhevsky & Hinton, 2009) presents a more challenging task of recognizing one of 10 different types of objects in a small image. The neural network used has the following layout: the input is a  $3 \times 32 \times 32$  image (i)  $3 \times 3$  linear convolution with stride of (1, 1) and 128 output maps, (ii)  $2 \times 2$  average pooling with (2, 2) stride (iii)  $3 \times 3$  convolution with (1, 1) stride and 83 maps (iv) Square activation (v)  $2 \times 2$  average pooling with (2, 2) stride (vi)  $3 \times 3$  convolution with (1, 1) stride and 163 maps (vii) Square activation (viii)  $2 \times 2$  average pooling with stride (2, 2)

<sup>8</sup>The accuracy is not reported in Boemer et al. (2018). However, they implement the same network as in Dowlin et al. (2016).



(viii) fully connected layer with 1024 outputs (ix) fully connected layer with 10 outputs (x) softmax. ADAM was used for optimization (Kingma & Ba, 2014) together with dropouts after layers (vii) and (viii). We use zero-padding in layers (i) and (vii). See Figure 3 for an illustration of the network.

For inference, adjacent linear layers were collapsed to form the following structure: (i)  $8 \times 8 \times 3$  convolutions with a stride of  $(2, 2, 0)$  and 83 maps (ii) square activation (iii)  $6 \times 6 \times 83$  convolution with stride  $(2, 2, 0)$  and 163 maps (iv) square activation (v) dense layer with 10 output maps. This network is much larger than the network used for MNIST by CryptoNets. The input to the CIFAR network has 3072 nodes, the first hidden layer has 16268 nodes and the second hidden layer has 4075 nodes (compared to 784, 845, and 100 nodes respectively for MNIST).<sup>9</sup> The accuracy of this network is 74.1% and it uses plain-text modulus  $p = 2148728833 \times 2148794369 \times 2149810177$  (the factors are combined using the Chinese Remainder Theorem) and  $n = 16384$ . See Figure 4 for an illustration of this network.

Due to the sizes of the hidden layers, implementing this network with SIMD representation requires more memory than available on the reference machine, since the SIMD representation requires a message for each node in each layer. Therefore, we used the LoLa-Conv approach to implement this network. The image is encoded using the convolution representation into  $3 \times 8 \times 8 = 192$  messages. The convolution layer is implemented using the convolution vector – row major matrix-vector multiplication technique. The results are combined into a single message using rotations and additions which allows the square activation to be performed with a single point-wise multiplication. The second convolution layer is performed using row major-dense vector multiplication. Although this layer is a convolution layer, each window of the convolution is so large that it is more efficient to implement it as a dense layer. The output is a sparse vector which is converted into a dense vector by point-wise multiplications and additions which allows the second square activation to be performed with a single point-wise multiplication. The last dense layer is implemented with a row major-dense vector technique again resulting in a sparse output.

Executing this network takes 730 seconds out of which the second layer consumes 711 seconds. Therefore, for this task the bottleneck in performance is the sizes of the weight matrices and data vectors as evident by the number of parameters which is  $< 90,000$  in the MNIST network and  $> 500,000$  in the CIFAR network. In the following section we present an approach to mitigate this problem.

## 5 Applying Deep Nets using Deep Representations

Homomorphic Encryption has two main limitations when used for evaluating deep networks: noise growth and message size growth. Noise growth is a result of the number of operations that has to take place. Each such operation increases the noise in the encrypted message and when this noise becomes too large, it is no longer possible to decrypt the message correctly. This problem can be mitigated using bootstrapping, while taking a performance hit. The message size grows with the size of the network as well. Since, in its core, the HE scheme operates in  $\mathbb{Z}_p$ , the parameter  $p$  has to be selected such that the largest number obtained during computation would be smaller than  $p$ . Since every multiplication might double the required size of  $p$ , it has to grow exponentially with respect to the number of layers in the network. The recently introduced HEAAN scheme (Cheon et al., 2017) is more tolerant towards message growth but even HEAAN would not be able to operate efficiently on very deep networks.

---

<sup>9</sup>The map counts of the different layers were selected such that the sizes of the hidden layers will fit inside the encrypted messages.

We propose solving both the message growth and the noise growth problems using deep representations. Instead of encrypting the data in its raw format, it is first converted, by a standard network, to create a deep representation. For example, if the data is an image, then instead of encrypting the image as an array of pixels, a network, such as AlexNet (Krizhevsky et al., 2012), VGG (Simonyan & Zisserman, 2014), or ResNet (He et al., 2016), first extracts a deep representation of the image, using one of its last layers. The resulting representation is encrypted and sent for evaluation. This approach has several advantages. First, this representation is small even if the original image is large. Moreover, with deep representations it is possible to obtain high accuracies using shallow networks: in most cases a linear predictor is sufficient which translates to a fast evaluation with HE. It is also a very natural thing to do since in many cases of interest, such as in medical image, training a very deep network from scratch is almost impossible since data is scarce. Hence, it is a common practice to use deep representation and train only the top layer(s) (Yosinski et al., 2014).

To test the deep representation approach we used AlexNet (Krizhevsky et al., 2012) to generate features and trained a linear model to make predictions on the CalTech-101 data-set (Fei-Fei et al., 2006).<sup>10</sup> See Table 4 for a summary of the data representations used for the CalTech-101 dataset. Since the CalTech-101 dataset is not class balanced, we used only the first 30 images from each class where the first 20 were used for training and the other 10 examples were used for testing. The obtained model has class-balanced accuracy of 75.7%. The inference time, on the encrypted data, takes only 0.178 seconds when using the dense vector – row major multiplication.

## 6 Conclusions

The problem of privacy in machine learning is gaining importance due to legal requirements and greater awareness to the benefits and risks of machine learning systems. The task of private inference, specifically with neural networks, serves as a benchmark and catalyst to promote further study in this domain. In this work, we showed how data representations can be used to accelerate private predictions using Homomorphic Encryption. We demonstrated both the ability to operate on more complex networks as well as lower latency on networks that were already studied in the past.

Some of the methods we propose require precomputation on the client side. In many cases, HE is presented as a method to offload computation from a power-limited client to the cloud. However, this is not the only reason to use privacy preserving prediction services: in some applications the data is sensitive while the service provider is not willing to share the model which may be a result of a costly development process. In these cases, the techniques we present here allow the provider to offer its services while respecting the privacy of data.

## References

- Martin Albrecht, Melissa Chase, Hao Chen, Jintai Ding, Shafi Goldwasser, Sergey Gorbunov, Jeffrey Hoffstein, Kristin Lauter, Satya Lokam, Daniele Micciancio, et al. Homomorphic encryption standard. 2018.
- Fabian Boemer, Yixing Lao, and Casimir Wierzynski. ngraph-he: A graph compiler for deep learning on homomorphically encrypted data. *arXiv preprint arXiv:1810.10121*, 2018.

---

<sup>10</sup>More complex classifiers did not improve accuracy.

- Florian Bourse, Michele Minelli, Matthias Minihold, and Pascal Paillier. Fast homomorphic evaluation of deep discretized neural networks. Technical report, Cryptology ePrint Archive, Report 2017/1114, 2017.
- Zvika Brakerski and Vinod Vaikuntanathan. Efficient fully homomorphic encryption from (standard) lwe. *SIAM Journal on Computing*, 43(2):831–871, 2014.
- Zvika Brakerski, Craig Gentry, and Vinod Vaikuntanathan. (leveled) fully homomorphic encryption without bootstrapping. *ACM Transactions on Computation Theory (TOCT)*, 6(3):13, 2014.
- Guoxing Chen, Sanchuan Chen, Yuan Xiao, Yinqian Zhang, Zhiqiang Lin, and Ten H Lai. Sgxpectre attacks: Leaking enclave secrets via speculative execution. *arXiv preprint arXiv:1802.09085*, 2018.
- Jung Hee Cheon, Andrey Kim, Miran Kim, and Yongsoo Song. Homomorphic encryption for arithmetic of approximate numbers. In *International Conference on the Theory and Application of Cryptology and Information Security*, pp. 409–437. Springer, 2017.
- Nathan Dowlin, Ran Gilad-Bachrach, Kim Laine, Kristin Lauter, Michael Naehrig, and John Wernsing. Cryptonets: Applying neural networks to encrypted data with high throughput and accuracy. In *International Conference on Machine Learning*, pp. 201–210, 2016.
- Nathan Dowlin, Ran Gilad-Bachrach, Kim Laine, Kristin Lauter, Michael Naehrig, and John Wernsing. Manual for using homomorphic encryption for bioinformatics. *Proceedings of the IEEE*, 105(3):552–567, 2017.
- Junfeng Fan and Frederik Vercauteren. Somewhat practical fully homomorphic encryption. *IACR Cryptology ePrint Archive*, 2012:144, 2012.
- Li Fei-Fei, Rob Fergus, and Pietro Perona. One-shot learning of object categories. *IEEE transactions on pattern analysis and machine intelligence*, 28(4):594–611, 2006.
- Craig Gentry. Fully homomorphic encryption using ideal lattices. In *STOC*, volume 9, pp. 169–178, 2009.
- Oded Goldreich, Silvio Micali, and Avi Wigderson. How to play any mental game. In *Proceedings of the nineteenth annual ACM symposium on Theory of computing*, pp. 218–229. ACM, 1987.
- Kaiming He, Xiangyu Zhang, Shaoqing Ren, and Jian Sun. Deep residual learning for image recognition. In *Proceedings of the IEEE conference on computer vision and pattern recognition*, pp. 770–778, 2016.
- Chiraag Juvekar, Vinod Vaikuntanathan, and Anantha Chandrakasan. Gazelle: A low latency framework for secure neural network inference. *arXiv preprint arXiv:1801.05507*, 2018.
- Diederik P Kingma and Jimmy Ba. Adam: A method for stochastic optimization. *arXiv preprint arXiv:1412.6980*, 2014.
- Esmail Mohammadian Koruyeh, Khaled Khasawneh, Chengyu Song, and Nael Abu-Ghazaleh. Spectre returns! speculation attacks using the return stack buffer. In *12th USENIX Workshop on Offensive Technologies (WOOT 18)*. USENIX Association, 2018.
- Alex Krizhevsky and Geoffrey Hinton. Learning multiple layers of features from tiny images. Technical report, Citeseer, 2009.

- Alex Krizhevsky, Ilya Sutskever, and Geoffrey E Hinton. Imagenet classification with deep convolutional neural networks. In *Advances in neural information processing systems*, pp. 1097–1105, 2012.
- Yann LeCun, Corinna Cortes, and Christopher JC Burges. Mnist handwritten digit database. at&labs, 2010.
- Frank McKeen, Ilya Alexandrovich, Alex Berenzon, Carlos V Rozas, Hisham Shafi, Vedvyas Shanbhogue, and Uday R Savagaonkar. Innovative instructions and software model for isolated execution. *HASP@ ISCA*, 10, 2013.
- M Sadegh Riazi, Christian Weinert, Oleksandr Tkachenko, Ebrahim M Songhori, Thomas Schneider, and Farinaz Koushanfar. Chameleon: A hybrid secure computation framework for machine learning applications. In *Proceedings of the 2018 on Asia Conference on Computer and Communications Security*, pp. 707–721. ACM, 2018.
- Amartya Sanyal, Matt J Kusner, Adrià Gascón, and Varun Kanade. Tapas: Tricks to accelerate (encrypted) prediction as a service. *arXiv preprint arXiv:1806.03461*, 2018.
- Karen Simonyan and Andrew Zisserman. Very deep convolutional networks for large-scale image recognition. *arXiv preprint arXiv:1409.1556*, 2014.
- Florian Tramer and Dan Boneh. Slalom: Fast, verifiable and private execution of neural networks in trusted hardware. *arXiv preprint arXiv:1806.03287*, 2018.
- Andrew C Yao. Protocols for secure computations. In *Foundations of Computer Science, 1982. SFCS'08. 23rd Annual Symposium on*, pp. 160–164. IEEE, 1982.
- Jason Yosinski, Jeff Clune, Yoshua Bengio, and Hod Lipson. How transferable are features in deep neural networks? In *Advances in neural information processing systems*, pp. 3320–3328, 2014.

## A Rotations

For the rotation operation in the BFV encryption scheme it is easier to think of the message as a  $2 \times n/2$  matrix:

$$\begin{bmatrix} m_1 & m_2 & \cdot & \cdot & m_{n/2} \\ m_{n/2+1} & m_{n/2+2} & \cdot & \cdot & m_n \end{bmatrix}$$

with this representation in mind, there are two rotations allowed, one switches the row, which will turn the above matrix to

$$\begin{bmatrix} m_{n/2+1} & m_{n/2+2} & \cdot & \cdot & m_n \\ m_1 & m_2 & \cdot & \cdot & m_{n/2} \end{bmatrix}$$

and the other rotates the columns. For example, rotating the original matrix by one column to the right will result in

$$\begin{bmatrix} m_{n/2} & m_1 & \cdot & \cdot & m_{n/2-1} \\ m_n & m_{n/2+1} & \cdot & \cdot & m_{n-1} \end{bmatrix}.$$

Since  $n$  is a power of two, and the rotations we are interested in are powers of two as well, for the sake of this work, thinking about the rotations as simple rotations of the elements in the message yields similar results. In this view, the row-rotation is a rotation of size  $n/2$  and smaller rotations are achieved by column rotations.

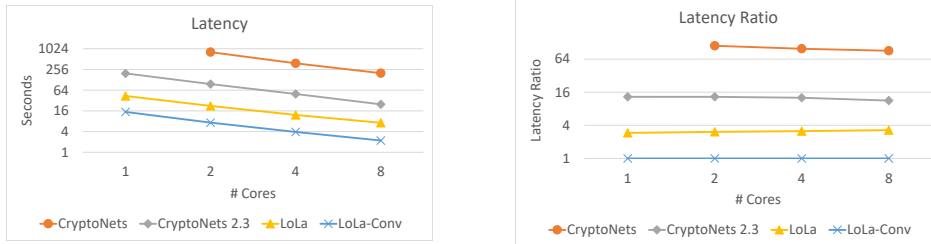


Figure 1: The latency of the different network implementations for the MNIST task with respect to the number of available cores. The right figure shows the ratio between the latency of each solution and the latency of the LoLa-Conv

## B The SIMD Representation

The vector structure of messages used by CryptoNets allow parallel execution over multiple data simultaneously. CryptoNets takes  $n$  input vectors  $\mathbf{v}^1, \dots, \mathbf{v}^n$  and creates a dense representation in which these  $n$  messages of length  $k$  are encoded in  $k$  messages  $\mathbf{m}^1, \dots, \mathbf{m}^k$  such that  $m_i^j = v_j^i$ . All operations between vectors and matrices are implemented using additions and multiplications only. For example, a dot product between two vectors of length  $k$  is implemented by  $k$  multiplications and additions. Therefore, it acts as a sparse representation.

The advantage of this representation, which we call the *SIMD Representation*, is that the cost of applying an operation to a vector is the same cost of applying the same operation to  $n$  vectors, hence it supports the Single Instruction Multiple Data (SIMD) framework. However, it is costly in two ways: the computational complexity of multiplying a matrix of size  $r \times k$  with a vector of length  $k$  is  $O(rk)$  HE operations, and the memory consumption is large as well since a vector of length  $k$  requires  $k$  messages. In this sense it is similar to the sparse representation. However, the ability to perform SIMD operations provides it with high throughput, much like the dense representation.

## C Parallel Scaling

The performance of the different solutions is affected by the amount of parallelism allowed. The hardware used for experimentation in this work has 8 cores. Therefore, we tested the performance of the different solutions with 1, 2, 4, and 8 cores to see how the performance varies. The results of these experiments are presented in Figure 1. These results show that at least up to 8 cores the performance of all methods scales linearly when tested on the MNIST data-set. This suggests that the latency can be further improved by using machines with higher core count.

## D LoLa representation changes

The following tables show the different stages that the data goes through when using LoLa. This illustrates how the different representations are used during the computation. Table 2 shows the

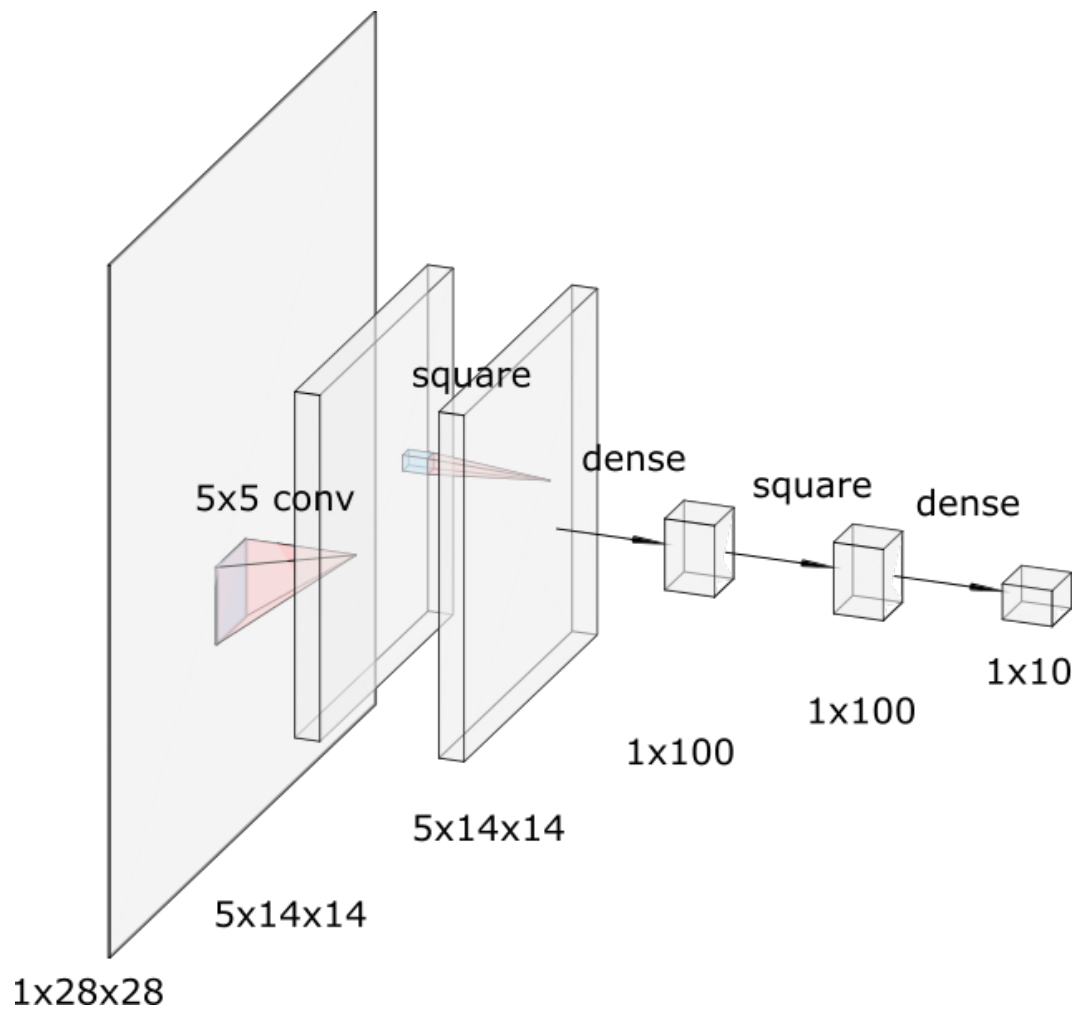


Figure 2: The structure of the network used for MNIST classification

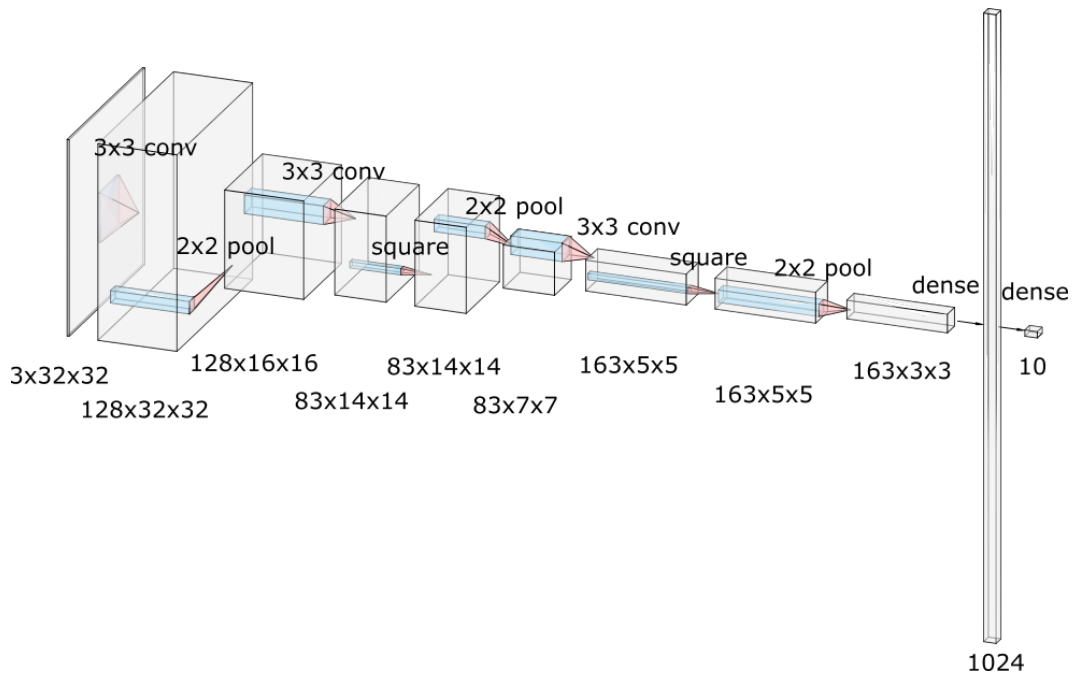


Figure 3: The structure of the network used for CIFAR classification.

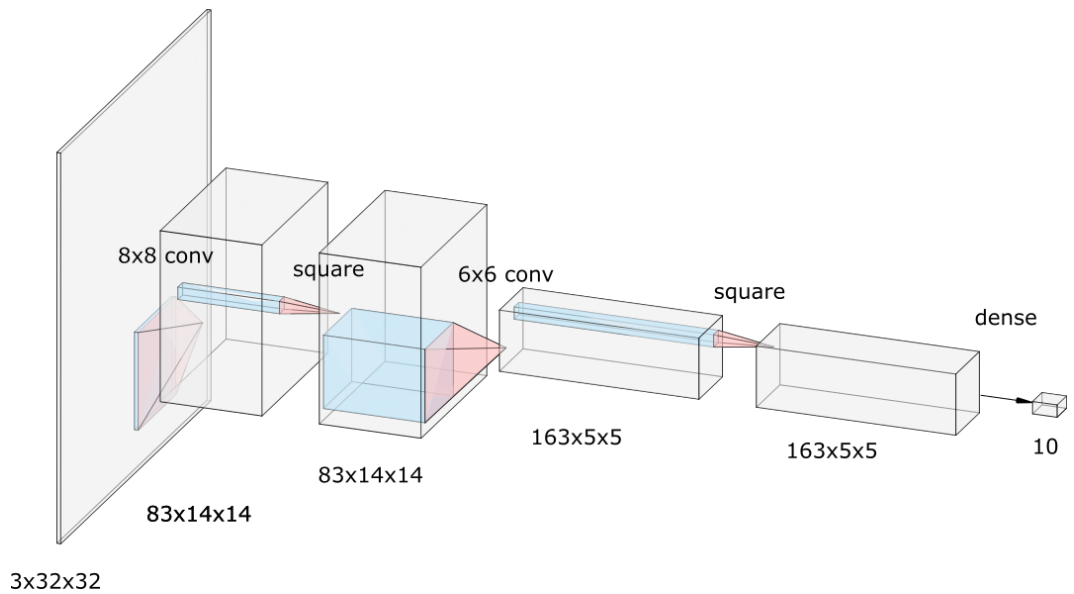


Figure 4: The structure of the network used for CIFAR classification after collapsing adjacent layers.

process that LoLa applies, Table 3 shows the process for LoLa-Conv, and Table 4 shows the process for the method proposed for processing the CalTech-101 dataset.



Layer	Input size	Weights format	Output format	Description
Encryption	784		dense	image is encrypted into a single message
5 × 5 convolution layer	784		convolution-interleave	mask input to create 25 messages
	25 × 169	convolution(column-major)	interleave	
square layer	5 × 169		interleave	combine 5 messages into one
	845		interleave	
dense layer	845		stacked-interleave	stack 16 copies
	16 × 845	row-major(stacked)	interleave	output in 7 messages
square layer	7 × 16		interleave	combine 7 messages into one
	100		interleave	
dense layer	100	row-major	sparse	

Table 2: LoLa data representation changes. The table shows the different formats of the data during its evaluation with LoLa-Conv

Layer	Input size	Weights format	Output format	Description
Preprocess	784		convolution	
Encryption	$25 \times 169$		convolution	image is encrypted into 25 messages
5 × 5 convolution layer	$25 \times 169$	convolution(column-major)	dense	output is in 5 dense messages
	$5 \times 169$		dense	combine 5 messages into one
square layer	845		dense	
dense layer	845		stacked	stack 8 copies
	$8 \times 845$	row-major(stacked)	interleave	output in 13 messages
	$13 \times 8$		interleave	combine 13 messages into one
square layer	100		interleave	
dense layer	100	row-major	sparse	

Table 3: LoLa-Conv data representation changes. The table shows the different formats of the data during its evaluation with LoLa

<b>Layer</b>	<b>Input size</b>	<b>Weights format</b>	<b>Output format</b>	<b>Description</b>
Preprocess	$200 \times 300$		dense	apply convolution layers from Alex-Net
Encryption	1000		dense	image is encrypted into 1 message
dense layer	1000	row-major	sparse	

Table 4: LoLa-CalTech data representation changes. The table shows the different formats of the data during its evaluation with LoLa on the CalTech-101 dataset